

Article

# Seasonal and Spatial Variation of Mo Isotope Compositions in Headwater Stream of Xijiang River Draining the Carbonate Terrain, Southwest China

Jie Zeng , Guilin Han \*  and Jian-Ming Zhu

Institute of Earth Sciences, China University of Geosciences (Beijing), Beijing 100083, China; zengjie@cugb.edu.cn (J.Z.); jmzhu@cugb.edu.cn (J.-M.Z.)

\* Correspondence: hanguilin@cugb.edu.cn; Tel.: +86-10-8232-3536; Fax: +86-10-8232-1115

Received: 1 May 2019; Accepted: 20 May 2019; Published: 23 May 2019



**Abstract:** The dissolved molybdenum (Mo) contents and Mo isotope in water samples from the upper Xijiang River (XJR), draining the carbonate terrain, southwest China, are reported to investigate the seasonal and spatial variations, sources, ion budget, and isotopic fractionation of dissolved Mo. The results show that the Mo concentrations (5.3–18.9 nmol/L) exhibit an extensive variation along the mainstream without significant spatial pattern, but the Mo concentrations are slightly higher in the dry season than in the wet season caused by the dilution effect. There is a slight spatial tendency for  $\delta^{98/95}\text{Mo}$  to become higher along the mainstream (0.51–1.78%), while the seasonal variations in  $\delta^{98/95}\text{Mo}$  values of NPR (Nanpanjiang River) reach and BPR (Beipanjiang River) reach can be identified higher in the dry season but lower in the wet season. Based on the hydro-geochemical analysis, the sources of dissolved Mo are identified as the carbonates and sulfide/sulfate minerals weathering with a seasonal contribution. Moreover, our results suggest there is no significant Mo isotopic fractionation during weathering and riverine transportation. The calculation of Mo budget demonstrates that the dissolved  $\delta^{98/95}\text{Mo}$  of river draining the carbonate terrain is underestimated, which could significantly influence the redox history of oceans by Mo isotope model.

**Keywords:** dissolved Mo; Mo isotope compositions; Xijiang River; Southwest China

## 1. Introduction

In the last few decades, isotope hydrology has developed from the application of analytical techniques or methods in physics to problems of Earth and environmental science. As a genuinely interdisciplinary science, isotope hydrology provides an effective integrated multidisciplinary approach to address the scientific and societal issues regarding water resources under natural and anthropogenic conditions (including climatic change) [1]. Hydrogen and oxygen stable isotopes ( $^2\text{H}$  and  $^{18}\text{O}$ ) are the classical tools of isotope hydrology, which are widely applied in the hydrological cycle and its processes [2,3]. With the rapid development of analytical techniques, many more methods were joined to the toolbox of isotope hydrologists, such as carbon isotopes in the evolutionary process of geothermal water and the carbon cycle of reservoir system [4,5], the applications of the strontium stable isotopes ( $^{87}\text{Sr}/^{86}\text{Sr}$  isotopic ratio) in surface and groundwater systems [6–9], and the nitrogen ( $\delta^{15}\text{N}$ ) and sulfur stable isotopes ( $\delta^{34}\text{S}$ ) in tracing water pollution and its sources [10–13]. However, the application of non-traditional stable isotopes (e.g.,  $\delta^{98/95}\text{Mo}$ ) in isotope hydrology is rarely reported up to now.

Molybdenum (Mo) is a metal with seven naturally occurring isotopes:  $^{92}\text{Mo}$  (14.84%),  $^{94}\text{Mo}$  (9.25%),  $^{95}\text{Mo}$  (15.92%),  $^{96}\text{Mo}$  (16.68%),  $^{97}\text{Mo}$  (9.55%),  $^{98}\text{Mo}$  (24.13%),  $^{100}\text{Mo}$  (9.63%) [14]. Mo is one of the most abundant transition metals in the ocean and is very sensitive to changes in redox conditions [15,16]. Recently, Mo isotope systematics has become increasingly important as a new proxy

for the redox history of the oceans and atmosphere [17,18]. Archer and Vance [19] suggested that the isotopic composition of riverine Mo varied from 0.2 to 2.3‰ and Mo concentrations varied from 2 nM to 511 nM. Previous studies showed that lighter Mo is preferentially adsorbed by weathering products or organic matter, but heavier Mo is transported by river water [15,19,20]. However, the details of the fractionation mechanism are still poorly known. Moreover, the studies of globally significant rivers have shown that the  $\delta^{98/95}\text{Mo}$  ratios ranged from 0.15 to 2.40‰ [15,16,19,21]. Pearce et al. [16] evaluated the isotope fractionation during transport from source to sink. Hammond [22] suggested that Mo exists in lubricants and fertilizers, but the effect on Mo isotope systematics in anthropogenic inputs has not been studied sufficiently.

The riverine Mo and Mo isotope could be affected by many factors, such as anthropogenic pollution, catchment geology, seasonal variations in river flow, and within-fluvial precipitation. Neubert et al. [21] assessed the influence of these factors on riverine Mo isotope and suggested that the variations in  $\delta^{98/95}\text{Mo}$  are mainly controlled by catchment lithology, particularly by weathering of sulfates and sulfides. By contrast, anthropogenic inputs affect neither the dissolved Mo isotopic composition nor the Mo concentration in the rivers, and the seasonal variations are also negligible [21]. The importance of weathering and river transport for Mo and Mo isotope behavior has also been confirmed in the river draining the basaltic terrain [16]. However, the seasonal variations in  $\delta^{98/95}\text{Mo}$  values observed in the Nile River are not negligible [19]. Therefore, identifying and understanding the processes which results in Mo isotope fractionation during weathering and riverine transport is essential for the quantitative application of this isotope system to study natural hydrological processes and anthropogenic inputs in the catchment.

Previous investigations have used major elements, hydrogen and oxygen isotope, carbon isotope, strontium isotope geochemical data to assess the chemical weathering rates, hydro-geochemical characteristics [2,23–27] in Xijiang River (XJR) system. However, the spatial and seasonal variations in the Mo isotope within these rivers are not well known. In this study, we have carried out a systematic investigation on the hydro-geochemistry of the headwater streams of XJR, particularly presented the  $\delta^{98/95}\text{Mo}$  ratios and their controlling factors for the river waters draining the typical carbonate catchments in Guizhou Province, southwest China. These catchments are essentially mono-lithological; consequently, there is little isotope variation from the weathering of different rock types. Rather, they provide an opportunity to study the effects of weathering processes accompanying variations in rainfall, soil, and riverine transportation, and provide the acceptable end-member value of Mo isotope in rivers draining the carbonate terrain.

## 2. Materials and Methods

### 2.1. Study Area

Guizhou Province is located in the center of the southeast Asian Karst Region, which forms part of the largest karst area in the world, underlain by limestone and dolomite [25]. The study area is in the upstream of XJR, including Nanpanjiang, Beipanjiang, and Hongshuihe River. The headstream tributaries were chosen as a target here because carbonate rocks terrain is widely distributed. The 914-km-long Nanpanjiang River (NPR), as the mainstream of the XJR, winds through Yunnan, Guizhou, and Guangxi provinces, draining an area of 56,880 km<sup>2</sup>. Beipanjiang River (BPR) is the largest tributary of the XJR, drains a 444 km transect crosses the Yunnan, Guizhou, and Guangxi Provinces, with a drainage area of 26,590 km<sup>2</sup> (Figure 1). Hongshuihe River (HSR) is the mainstream reach of the XJR after the BPR flows into the NPR.

Under the influence of a warm subtropical climate, the Beipanjiang, Nanpanjiang and Hongshuihe River catchments have an average annual air temperature of 14 to 22 °C in the entire drainage basin [26,28]. Mean annual precipitation, averaged over several years, is from 800 to 1200 mm and the precipitation decreases from south-east to north-west. The precipitation is concentrated in the wet season (June to September) and accounts for about 50–55% of the total annual precipitation.

The elevation gradients of the study area are abrupt, and the altitudes of the river catchments are about 2400 m in its riverhead and about 240 m at lower reaches. Vegetation covers of the different area are variable, generally with higher vegetation covers in their lower reaches. Anthropogenic pressure is considerable as about 30 million people live in Guizhou Province. The land deforestation has significantly enhanced soil erosion.

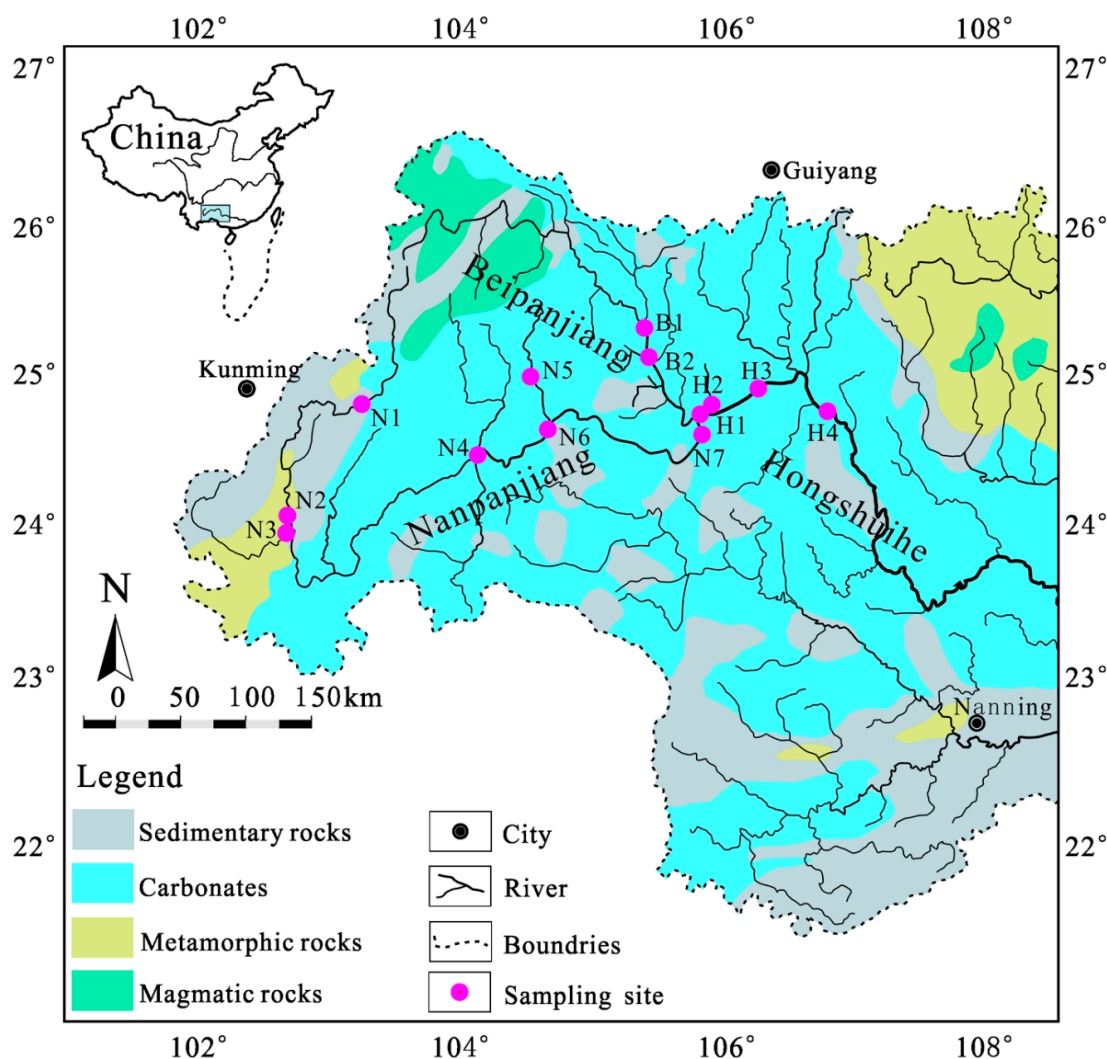


**Figure 1.** Map showing the lithology and sampling locations of the upper Xijiang River.

## 2.2. Sampling and Chemical Analysis

Two water samples from BPR (B1 and B2), seven water samples from NPR (N1 to N7) and four water samples from HSR (H1 to H4) were collected in July of 2014 during the wet season and in January of 2015 during the dry season. The sampling sites are shown in Figure 1. Further details on the collection and previous analyses of these samples, including cation and anion, can be found elsewhere [2,26,27]. The concentrations of dissolved trace elements were determined by inductively coupled plasma-mass spectrometry (ICP-MS, Elan DRC-e, Perkin Elmer, Waltham, MA, USA) at the Institute of Geographic Sciences and Natural Resources Research, Chinese Academy of Sciences [29]. Chinese standard reference materials (GSB 04-1767-2004) were used to perform the method validation and quality control. Reagent and procedural blanks were analyzed in parallel with samples which were treated by identical procedures. The drift of the calibration curve was monitored by analyses of the quality control standards before, during, and after the analysis of each set of samples.

### 2.3. Analytical Technique for Mo Isotope Composition

The Mo isotope composition of the river water was measured using the double spike method of Li et al. [30]. The  $^{97}\text{Mo}$  and  $^{100}\text{Mo}$  double spikes were added to each sample prior to chemical purification. In the mixtures, the majority of  $^{97}\text{Mo}$  and  $^{100}\text{Mo}$  are derived from the spikes while the bulk of  $^{98}\text{Mo}$ ,  $^{96}\text{Mo}$ , and  $^{95}\text{Mo}$  come from samples. Thus, based on the measured  $^{98}\text{Mo}/^{97}\text{Mo}$ ,  $^{96}\text{Mo}/^{97}\text{Mo}$ ,  $^{95}\text{Mo}/^{97}\text{Mo}$  and the  $^{100}\text{Mo}/^{97}\text{Mo}$  ratio in the spike, the Mo isotope fractionation during instrumental analysis (mass-bias of Mass-Spectrometer) and chemical purification (e.g., column chemistry) can be corrected.

During the chemical purification, water samples containing Mo were dried down firstly and then dissolved in nitrohydrochloric acid ( $\text{HCl}:\text{HNO}_3 = 3:1$ ) before being passed through Bio-Rad AG-MP1M (Hercules, CA, USA) (100–200) resin, using 7 N HCl as eluent solutions. Then passed through Bio-Rad® AG50W-X8 (Hercules, CA, USA) (200–400) resin using 1.4 N HCl as eluent solutions. All the above chemical treatments were carried out in the 100-class clean room in the Surficial Environment Geochemistry Laboratory, China University of Geosciences, Beijing, China. After the separation and purification of Mo from the samples.

Mo isotopic ratios were determined using a multiple collector inductively coupled plasma-mass spectrometry (MC-ICP-MS, Nu II, UK) at the Institute of Geochemistry, Chinese Academy of Science, Guiyang, China.

The isotopic ratio of Mo was expressed as  $\delta^{98/95}\text{Mo}$  notation as follows:

$$\delta^{98/95}\text{Mo} = [({}^{98}\text{Mo}/{}^{95}\text{Mo})_{\text{sample}}/({}^{98}\text{Mo}/{}^{95}\text{Mo})_{\text{SRM3134}} - 1] \times 1000 \quad (1)$$

where SRM 3134 is the international Mo isotope standard. The precision of our measurements was expressed as two standard deviations (2 SD) of the mean values determined by repeated sample measurements. Over the course of this study, the mean  $\delta^{98/95}\text{Mo}$  value for SRM 3134, IAPSO, and Atlantic Seawater 8.6 (HSQ) were determined to be  $-0.19 \pm 0.07\text{‰}$  (2 SD,  $n = 20$ ),  $2.09 \pm 0.08\text{‰}$  (2 SD,  $n = 20$ ) and  $2.05 \pm 0.08\text{‰}$  (2 SD,  $n = 20$ ) while the total Mo in blank samples was less than 0.2 ng (ca. 0.3%).

### 3. Results

The hydrological parameters, chemical composition of major ions, dissolved Mo concentrations and Mo isotope compositions of river water are shown in Table 1. Spatial and seasonal patterns of dissolved Mo and Mo isotope compositions are also shown in Table 1. These findings suggest that periodic sampling of headwaters provides valuable information about solute sources and sub-catchment resilience to disturbance. The pH varied from 7.6 to 8.4 in the wet season and 7.8 to 8.3 in dry season, respectively, while the EC in the wet season (155–267  $\mu\text{S}/\text{cm}$ ) were significantly lower than that in the dry season (370–602  $\mu\text{S}/\text{cm}$ ). The variations in DO were quite significant (4.9–12.4 mg/L) due to the large difference of water flow velocity in the wet season, while the variations in DO were relatively weak in the dry season (6.6–9.2 mg/L). The most abundant cation in the river water was  $\text{Ca}^{2+}$ , accounting for 50–76% of the total cations in the two sampling periods, with concentrations ranging from 1.03–2.09 mmol/L in the wet season and 0.80–1.88 mmol/L in the dry season, respectively. The concentrations of  $\text{Na}^+$ ,  $\text{K}^+$  and  $\text{Mg}^{2+}$  ranged from 0.13 to 0.92 mmol/L, 0.04 to 0.18 mmol/L and 0.36 to 0.81 mmol/L, respectively. The concentration of  $\text{HCO}_3^-$  (ranged from 1.84 to 3.70 mmol/L) accounting for over 53% of the total anions, while the concentrations of  $\text{Cl}^-$ ,  $\text{NO}_3^-$  and  $\text{SO}_4^{2-}$  ranged from 0.11 to 0.73 mmol/L, 0.06 to 0.56 mmol/L and from 0.30 to 0.86 mmol/L, respectively.

**Table 1.** Hydrological parameters, Mo concentrations and  $\delta^{98/95}\text{Mo}$ , major ions of the upper Xijiang River water.

Sample	pH <sup>a</sup>	T <sup>a</sup>	EC <sup>a</sup>	DO <sup>a</sup>	Mo <sup>a</sup>	$\delta^{98/95}\text{Mo}$	Na <sup>+</sup>	K <sup>+</sup>	Mg <sup>2+</sup>	Ca <sup>2+</sup>	HCO <sub>3</sub> <sup>-</sup>	Cl <sup>-</sup>	NO <sub>3</sub> <sup>-</sup>	SO <sub>4</sub> <sup>2-</sup>	
		°C	µS/cm	mg/L	nmol/L	‰	mmol/L <sup>b</sup>								
Wet season															
N1	7.6	21.3	249	4.9	5.7	0.87	0.45	0.12	0.63	1.79	3.29	0.48	0.29	0.50	
N2	7.8	22.7	267	6.9	8.8	0.77	0.23	0.11	0.68	2.09	3.27	0.44	0.45	0.50	
N3	8.1	23.3	259	7.1	8.2	0.51	0.56	0.18	0.79	1.59	2.84	0.56	0.41	0.48	
N4	7.9	23.9	225	6.8	9.7	0.95	0.26	0.08	0.58	1.73	2.95	0.27	0.56	0.49	
N5	8.1	20.3	181	8.1	5.3	1.08	0.13	0.04	0.39	1.47	2.15	0.16	0.31	0.50	
N6	8.1	27.1	163	7.4	9.3	0.95	0.29	0.06	0.54	1.04	1.97	0.17	0.21	0.50	
N7	8.4	30.6	158	12.3	6.6	1.05	0.22	0.05	0.47	1.13	2.21	0.17	0.16	0.34	
H1	8.0	31.9	193	8.4	5.7	0.90	0.34	0.06	0.46	1.43	2.74	0.41	0.06	0.36	
H2	8.4	31.7	162	12.4	8.1	1.12	0.26	0.06	0.51	1.05	2.05	0.18	0.14	0.38	
H3	8.3	33.3	155	10.0	7.2	1.05	0.24	0.05	0.43	1.03	1.84	0.14	0.10	0.40	
H4	7.7	22.7	182	6.6	5.9	1.25	0.17	0.05	0.36	1.48	2.60	0.11	0.12	0.36	
B1	8.3	27.0	206	9.0	6.3	0.83	0.23	0.05	0.46	1.55	2.33	0.14	0.28	0.70	
B2	8.0	21.8	201	8.5	7.1	1.20	0.25	0.04	0.37	1.56	2.33	0.11	0.25	0.68	
Dry season															
N1	8.2	11.4	602	9.0	6.6	1.09	0.92	0.18	0.67	1.88	3.36	0.73	0.52	0.86	
N2	8.3	13.4	530	8.5	9.4	1.03	0.44	0.13	0.78	1.85	3.41	0.39	0.44	0.69	
N3	8.3	13.6	588	8.8	6.3	0.97	0.66	0.16	0.81	1.23	3.70	0.56	0.19	0.63	
N4	8.3	15.3	396	7.9	8.0	1.05	0.22	0.06	0.51	1.49	3.17	0.17	0.21	0.31	
N5	8.3	15.4	401	7.8	7.2	0.93	0.21	0.05	0.48	1.31	3.15	0.16	0.20	0.30	
N6	8.3	15.7	398	7.1	18.9	1.00	0.21	0.05	0.50	1.41	3.12	0.16	0.20	0.31	
N7	8.1	17.8	384	7.9	9.7	0.96	0.23	0.05	0.46	1.51	2.74	0.13	0.22	0.44	
H1	8.0	17.5	383	7.7	7.8	1.04	0.22	0.05	0.46	0.83	2.76	0.14	0.23	0.43	
H2	8.1	18.0	381	8.0	7.9	0.97	0.23	0.05	0.47	1.51	2.73	0.14	0.21	0.45	
H3	8.3	10.6	465	9.2	7.6	1.78	0.21	0.05	0.60	1.05	3.11	0.17	0.12	0.84	
H4	7.8	19.1	370	7.7	6.8	1.03	0.22	0.05	0.42	0.80	2.70	0.12	0.20	0.42	
B1	8.0	10.2	414	6.6	7.3	1.03	0.21	0.06	0.60	1.51	3.15	0.14	0.16	0.43	
B2	8.2	16.2	409	9.0	7.3	1.25	0.32	0.04	0.45	0.89	2.56	0.12	0.18	0.68	

Note: <sup>a</sup> Data are taken from [2,29]; <sup>b</sup> Major ion concentrations are calculated from [26,27]; T, temperature; EC, electric conductivity; DO, dissolved oxygen; Mo, molybdenum;  $\delta^{98/95}\text{Mo}$ , delta value of <sup>98</sup>Mo versus <sup>95</sup>Mo.

### 3.1. Seasonal and Spatial Variations in Mo Concentration

The dissolved Mo concentrations of the two sampling periods in the upper XJR are given in Table 1. The Mo concentrations of Nanpanjiang River varied between 5.3 and 9.7 nmol/L (with an average valued of 7.6 nmol/L) during the wet season, while between 6.3 and 18.9 nmol/L (with an average valued of 9.4 nmol/L) during the dry season. The Mo concentrations of BPR were 6.3 (B1) and 7.1 (B2) nmol/L during the wet season and 7.3 nmol/L of the two sites during the dry season. For the HSR, Mo concentrations varied between 5.7 nmol/L and 8.1 nmol/L (with an average value of 6.7 nmol/L) during the wet season, between 6.8 nmol/L and 7.9 nmol/L (with an average value of 7.5 nmol/L) during the dry season. The Mo concentrations in all samples are higher than the world river average value (4.4 nmol/L) [31], but the range of Mo concentrations are similar to the lower XJR (5.3–10.5 nmol/L) [15]. Along the mainstream of the upper XJR (N1–N7, H1–H4), the variation in Mo concentrations is extensive (Figure 2), with no significant pattern of spatial distribution. On the seasonal scale, the Mo concentrations of two sampling periods varied in a relatively narrow range (Figure 2), without significant difference (one-way analysis of variance,  $p < 0.05$ ). As shown in Figure 2, the Mo concentrations of most of the sites are slightly higher in the dry season than in the wet season, which is mainly controlled by the dilution effect during the wet season [29,32].

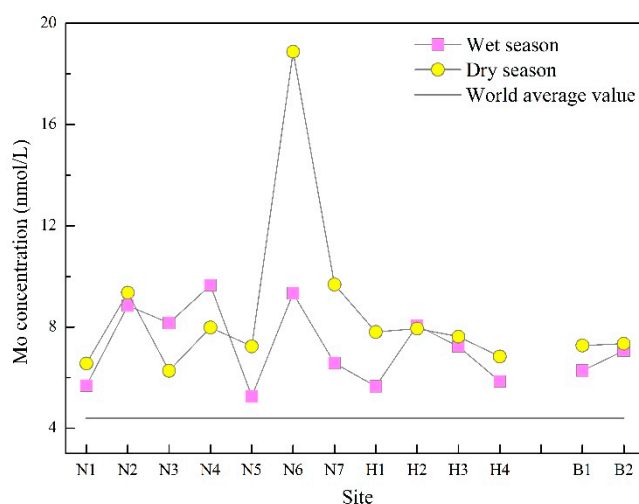


**Figure 2.** Seasonal and spatial variations in dissolved Mo concentrations of the upper Xijiang.

### 3.2. Mo Isotopic Composition

The dissolved Mo isotopic compositions ( $\delta^{98/95}\text{Mo}$ ) of the upper XJR vary between 0.51‰ and 1.78‰ (Table 1 and Figure 3), with an average of  $0.96 \pm 0.19\text{‰}$  (1 SD) in the wet season and  $1.09 \pm 0.22\text{‰}$  (1 SD) in the dry season, respectively. These  $\delta^{98/95}\text{Mo}$  values are within the ranges of the global river water reported in the previous studies (0.15‰ to 2.40‰, Figure 3a) [15,16,19,21,33,34]. As a river flowing through the essentially mono-lithological area (carbonate rock), the  $\delta^{98/95}\text{Mo}$  values of upper XJR water are significantly higher than that of the mean value of average basalts and granites (0.0‰ to 0.4‰) [19,35]. In contrast, the dissolved Mo isotopic compositions of upper XJR are slightly lower than that of the lower XJR (1.04‰ to 1.31‰) [15], except for the site H3 during the dry season (Figure 3a). It should be noted that the river waters from the NPR have lower  $\delta^{98/95}\text{Mo}$  ratios in comparison with the BPR and HSR during the two sampling periods (Figure 3b). As shown in Figure 3, although the  $\delta^{98/95}\text{Mo}$  values varied a very small range, the  $\delta^{98/95}\text{Mo}$  values are higher in the dry season but lower in the wet season of both NPR and BPR reaches, while the seasonal pattern of the  $\delta^{98/95}\text{Mo}$  values of HSR reach was not obvious. This seasonal variation in  $\delta^{98/95}\text{Mo}$  values is similar to the Nile River [19].

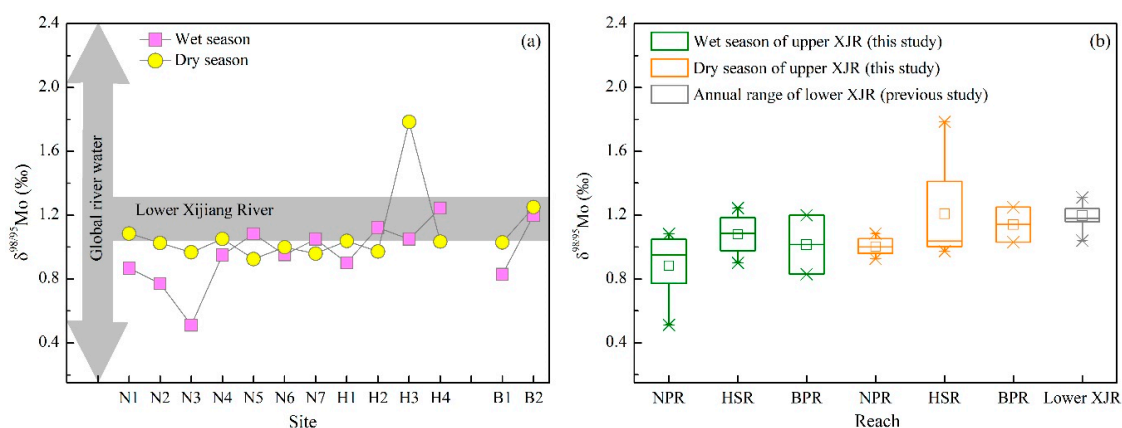


**Figure 3.** Seasonal and spatial variations in Mo isotopic composition of the upper Xijiang River; (a) the  $\delta^{98/95}\text{Mo}$  values along the upper XJR; (b) the box plot of  $\delta^{98/95}\text{Mo}$  values in different reaches of upper XJR.

## 4. Discussion

### 4.1. Source of Dissolved Mo in the River Water

The dissolved species of the river water are mainly derived from atmospheric inputs, anthropogenic sources and weathering of rocks [26,27].

#### 4.1.1. Atmospheric and Anthropogenic Inputs

Both the Mo concentration and  $\delta^{98/95}\text{Mo}$  of the Earth-surface system are influenced by the atmospheric input derived from rainwater and atmospheric dust, such as the topsoil in Hawaii [35], which is attributed to the Mo inputs from rainwater with generally higher  $\delta^{98/95}\text{Mo}$  than soil. However, Wang et al. suggested that the effect of Mo input from rainwater on  $\delta^{98/95}\text{Mo}$  variations in the topsoil is negligible [20]. Based on the analysis of trace element content and isotope, the atmospheric dust input to the current Earth-surface system is limited and its influence on  $\delta^{98/95}\text{Mo}$  is negligible, even though in the areas with loess deposition in North China [20]. In the catchment, the river water area only accounts for 0.72% of the basin area [36] and the direct Mo input to the river water through rainwater and atmospheric dust is far less than the Mo input to the soil. Moreover, the Mo content of the rainwater and atmospheric dust of karst region [37–40] are also relatively lower than that of economy developed region, such as the acid precipitation zone of southern China [41], Yangtze River Delta [42], Beijing [43], Chang-Zhu-Tan production region [44] and the Asian dust [45]. Consequently, we conclude that the effect of atmospheric input on Mo concentration in river water is limited and the influence on  $\delta^{98/95}\text{Mo}$  is negligible.

As for the anthropogenic inputs, coal industry and agricultural activities are the main anthropogenic sources of dissolved Mo in rivers [21]. Previous hydro-geochemical studies suggest that both the NPR and BPR are affected by urban sewage and agricultural activities, the BPR is more vulnerable by the coal industry [26,27]. However, there are no significant variation in Mo concentrations between NPR and BPR samples (Table 1 and Figure 2), except for the site N6 during the dry season (near a river transport dock but with a similar  $\delta^{98/95}\text{Mo}$  value to other sites). Additionally, an argument nonsupport agriculture as the predominant factor on Mo concentrations and  $\delta^{98/95}\text{Mo}$  is that the similar land-use (cultivated land account for 35% of basin area [36]) and farming practice of the entire upper XJR [10]. Therefore, the anthropogenic inputs could neither significantly increase the Mo concentration nor appreciably modify the Mo isotopic compositions.

#### 4.1.2. Weathering of Rock

Generally, dissolved Mo in river water primarily originated from the chemical weathering of the rocks and minerals exposed in the fluvial basins [15,16,21]. The results of principal component analysis

of dissolved elements in entire XJR basin also indicate that the Mo is greatly contributed by natural sources [29], i.e., rock weathering and subsequent pedogenesis [32]. As shown in Figure 1, carbonate is the dominant lithology of upper XJR [10], these catchments are essentially mono-lithology [28,46], consequently there may be little variation of Mo source contribution from the weathering of different rock types. The natural source of the dissolved Mo can be further identified by analyzing the Mo concentrations and the ions compositions of the river water. Gaillardet et al. suggest that  $\text{Ca}^{2+}$  in river water is mainly resulted from carbonate weathering, while  $\text{K}^+$  is mainly derived from the silicates weathering [47]. Although anthropogenic sulfuric acid emissions (such as acid rain) may significantly affect the content of  $\text{SO}_4^{2-}$  in river water, the  $\text{SO}_4^{2-}$  deposition in karst areas of southwest China has shown a decreasing trend with the implementation of environmental protection policies such as sulfur dioxide reduction [48,49] and the sulfide minerals weathering is the major source of  $\text{SO}_4^{2-}$  in the river water [24]. Consequently, the  $\text{K}^+$ ,  $\text{Ca}^{2+}$  and  $\text{SO}_4^{2-}$  concentrations of the river water were used to identify the Mo contribution from weathering of carbonates, silicates and sulfide/sulfate minerals. Since the discharge of upper XJR represents large seasonal variations [26,27,29], the raw data of the Mo,  $\text{K}^+$ ,  $\text{Ca}^{2+}$  and  $\text{SO}_4^{2-}$  concentrations (meq/L) in upper XJR are normalized by the total dissolved solids (TDS, meq/L) to reduce the influence of dilution effect. The Kolmogorov–Smirnov (K–S) test, as a non-parametric test, is applied to test the normal distribution of our data and the results showing that the data for correlation analysis are normally distributed during the both season and then Pearson correlation is meaningful.

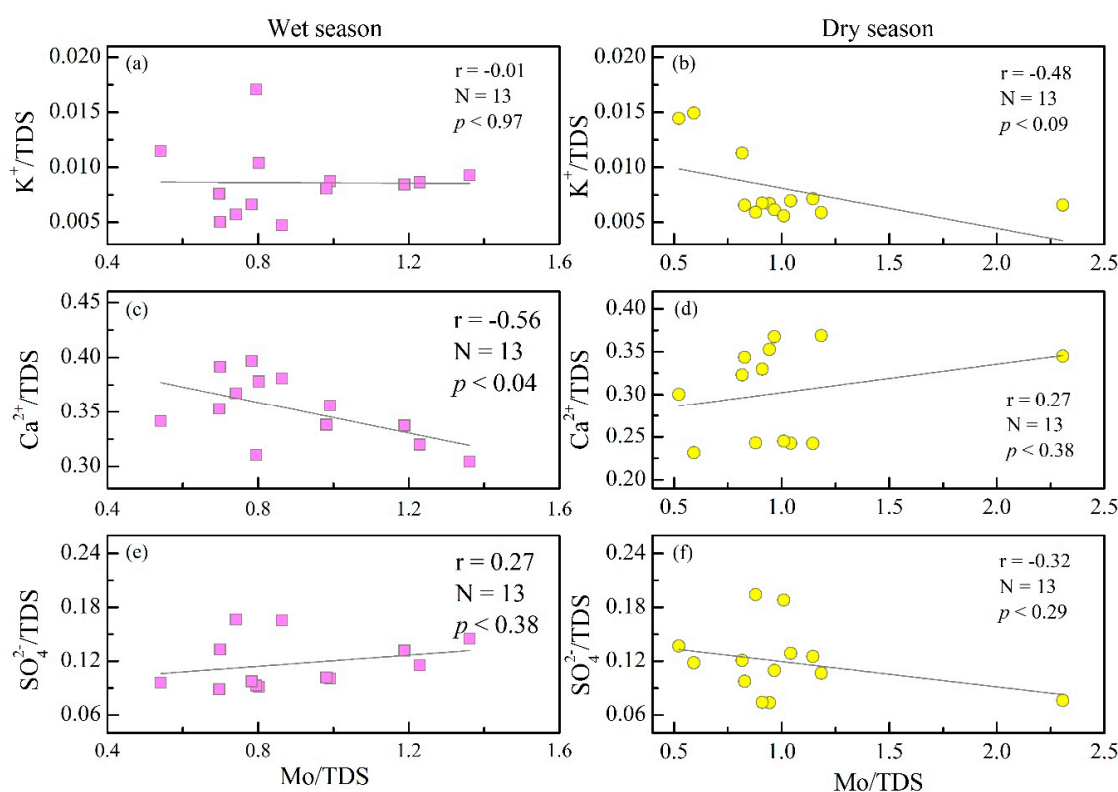


**Figure 4.** Correlations between Mo/TDS and  $\text{K}^+/\text{TDS}$ ,  $\text{Ca}^{2+}/\text{TDS}$  and  $\text{SO}_4^{2-}/\text{TDS}$  of upper XJR water; Mo/TDS versus  $\text{K}^+/\text{TDS}$  in wet season (a) and dry season (b); Mo/TDS versus  $\text{Ca}^{2+}/\text{TDS}$  in wet season (c) and dry season (d); Mo/TDS versus  $\text{SO}_4^{2-}/\text{TDS}$  in wet season (e) and dry season (f).

There is no clear correlation between Mo/TDS and  $\text{K}^+/\text{TDS}$  in the wet season, while a negative correlation in the dry season (Figure 4a,b), indicating that enhanced  $\text{K}^+$  input to the river water from the silicates weathering seems to be associated with a lower Mo input, particularly in the dry season. Therefore, silicate weathering is not the main source of dissolved Mo of the upper XJR water.

However,  $\text{Ca}^{2+}/\text{TDS}$  show statistically significant negative correlation with  $\text{Mo}/\text{TDS}$  in the wet season ( $r = -0.56$ ,  $p < 0.04$ ) and show a positive correlation in the dry season (Figure 4c,d). Conversely, the correlations between  $\text{Mo}/\text{TDS}$  and  $\text{SO}_4^{2-}/\text{TDS}$  in the two seasons are opposite to that between  $\text{Mo}/\text{TDS}$  and  $\text{Ca}^{2+}/\text{TDS}$ , i.e., a positive correlation in the wet season and a negative correlation in the dry season (Figure 4e,f). These results suggest that the carbonates and sulfide/sulfate minerals weathering contribute seasonally to the dissolved Mo in the upper XJR water. Specifically, the dissolved Mo is controlled by the carbonates weathering in the dry season, while the dissolved Mo in the wet season is controlled by the sulfide/sulfate minerals weathering. This is supported by the sulfide mineral deposits (such as pyrites) can generally be found in Yunnan and Guizhou provinces (upper XJR basin) [15,24,50]. Meanwhile, the seasonal variation of contribution of carbonates and sulfide/sulfate minerals weathering may be mainly controlled by the difference of weathering rate [24,25] and the Mo content of these rocks or minerals ( $<1 \mu\text{g/g}$  for carbonate rocks,  $10\sim 100 \mu\text{g/g}$  for sulfide minerals) [15,50,51]. Therefore, we conclude that the main sources of the dissolved Mo in the upper XJR are attributed to the carbonates and sulfide/sulfate minerals weathering.

#### 4.2. Mo Isotope Fractionation during Weathering and Riverine Transportation

Generally, the data from the two endmembers simple mixing show a clear negative correlation: high  $\delta^{98/95}\text{Mo}$  ratios are associated with high Mo concentrations [21], such as the mixing of estuary (Itchen River) between seawater with high Mo concentration and  $\delta^{98/95}\text{Mo}$  and a fluvial dissolved end-member with low Mo concentration and  $\delta^{98/95}\text{Mo}$  (Figure 5a) [19]. However, there are more than two endmembers mixed and/or more than one isotopic fractionation process if the relationship between Mo concentration and  $\delta^{98/95}\text{Mo}$  is non-linear. As shown in Figure 5b, compared to the lower XJR, the Mo concentration and  $\delta^{98/95}\text{Mo}$  in upper XJR water show an insignificant linear trend. As we previously noted that the sources of dissolved Mo in the upper XJR are carbonates and sulfide/sulfate minerals weathering. Thus, the fractionation process of Mo isotope needs a further discussion.

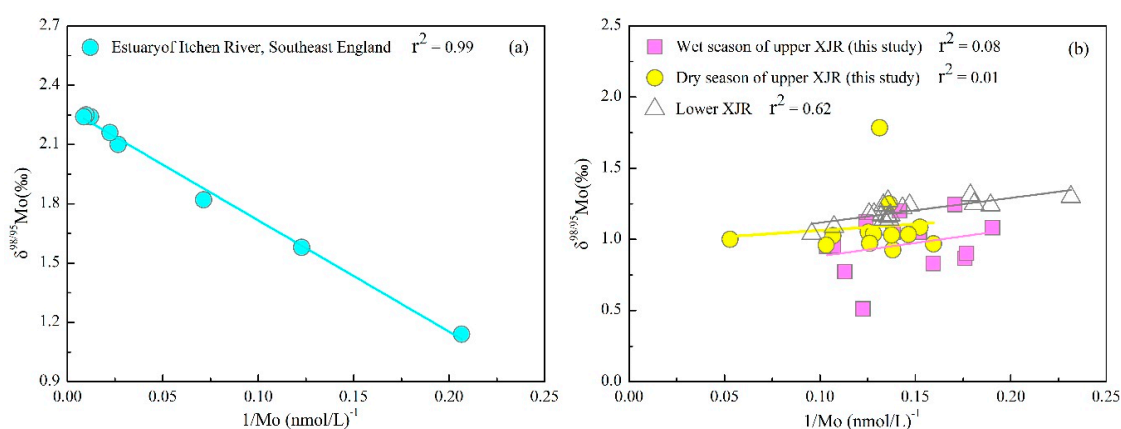


**Figure 5.** The correlation between  $\delta^{98/95}\text{Mo}$  and  $1/[\text{Mo}]$ , (a) the dissolved  $\delta^{98/95}\text{Mo}$  in the Itchen estuary versus  $1/[\text{Mo}]$  [19]; (b) the dissolved  $\delta^{98/95}\text{Mo}$  versus  $1/[\text{Mo}]$  for upper XJR water (this study) and lower XJR [15].

In the last decade, there has been significant work confirming the Mo isotopic fractionation in soil adsorption process as well as during river transport [21,52]. The lighter Mo could be trapped by organic matter and cause the isotope fractionation [21,53] and hence the isotopically light Mo preferentially adsorbed by weathering products (e.g., soil) [15,16,53]. As the less Mo from the soil releasing to the river, the  $\delta^{98/95}\text{Mo}_{\text{water}}$  of river water will increase and an opposite relationship will be observed between  $\delta^{98/95}\text{Mo}_{\text{water}}$  and Mo concentrations. The positive correlation between  $\delta^{98/95}\text{Mo}$  and  $1/[\text{Mo}]$  in both two seasons shown in Figure 5b indicates that the effect of soil capture on the Mo isotope fractionation is limited in the upper XJR water. This could be explained thus: although lighter Mo is

preferentially retained in soil, soil erosion will release them again. Therefore, if the integrated volume of soil formation and soil erosion are equal, the net Mo isotope effect will be zero [21]. Interestingly, the upper XJR is located in karst areas where soil erosion is extremely severe [26,54–56] and do not support long-term storage of lighter Mo in soils and result in a weak effect on Mo isotope fractionation. This is different from the Mo isotope study in the lower XJR, where the laterites are widely developed and the capacity for trapping Mo is apparently large [15].

Mo isotope fractionation is affected by several factors during the riverine transportation, such as redox condition, organic matter content, Fe/Mn oxyhydroxide particles suspended in the water. Neubert et al. [21] suggests that the isotope fractionation of dissolved Mo could be occurred in suboxic conditions (e.g., swamps), but do not significantly influence the  $\delta^{98/95}\text{Mo}_{\text{water}}$ . In this study, the high DO values (up to 12.4 mg/L, Table 1) of all the water samples in upper XJR, indicating an aerobic environment and the correlation between DO and  $\delta^{98/95}\text{Mo}$  is also insignificant (Table 2). Thus, the effect of redox condition on Mo isotope fractionation is limited.

**Table 2.** The correlation between  $\delta^{98/95}\text{Mo}$ , DO,  $\text{Fe}_{\text{SPM}}$ ,  $\text{Mn}_{\text{SPM}}$ , and DOC for upper Xijiang River water.

Item		DO	$\text{Fe}_{\text{SPM}}^a$	$\text{Mn}_{\text{SPM}}^a$	DOC <sup>b</sup>
$\delta^{98/95}\text{Mo}$	Pearson correlation	0.31	−0.69	−0.72	−0.66
	significance (two-tailed)	0.12	0.31	0.28	0.05
	N	26	4	4	9

Note: <sup>a</sup>  $\text{Fe}_{\text{SPM}}$  and  $\text{Mn}_{\text{SPM}}$  concentrations (in  $\mu\text{g/L}$ ) are from [57] in NPR and BPR (only four sites: N1, N2, N4 and B2, in wet season); <sup>b</sup> DOC concentrations (in mg/L) are from [58] in NPR and BPR (N1–N7, B1, and B2, wet season); DO, dissolved oxygen;  $\text{Fe}_{\text{SPM}}$ , Fe in suspended particulate matter (SPM);  $\text{Mn}_{\text{SPM}}$ , Mn in suspended particulate matter; DOC, dissolved organic carbon; N, sample size.

For the Fe/Mn oxyhydroxide in suspended particulate matter (SPM),  $\delta^{98/95}\text{Mo}$  values has been reported to be generally negative in Fe-precipitates (between −0.65 and 0.07‰) [16], indicate that Fe/Mn oxyhydroxide are preferentially adsorbed light Mo isotopes. However, the negative correlation between  $\delta^{98/95}\text{Mo}_{\text{water}}$  and  $\text{Fe}_{\text{SPM}}$  (or  $\text{Mn}_{\text{SPM}}$ ) in upper XJR (Table 2) does not support the above view, i.e., the adsorption of SPM within the upper XJR cannot be driving the dissolved load to heavier Mo [21]. Furthermore, although the  $\delta^{98/95}\text{Mo}$  values of NPR waters are lower than that of HSR overall (Figure 3b), but the downstream fractionation is not significant within the whole upper XJR (Figure 3a). Organic matter adsorption, as another possible cause of fractionation [21], the significant negative correlation between  $\delta^{98/95}\text{Mo}_{\text{water}}$  and DOC ( $r = -0.66$ ,  $p < 0.05$ , Table 2), which could explain the slightly variation of Mo isotopes from NPR to HSR (Figure 3a).

In summary, the Mo isotopic fractionation during weathering and riverine transportation is not significant in upper XJR.

#### 4.3. Consequences of River in Carbonate Terrain for the Global Mo Isotope Budget

The previous studies have tended to make a key assumption when applying the Mo isotope record of marine sediments to reconstruct the redox conditions of ancient oceans [15,17,18]. This assumption is that the Mo isotopic composition of the terrestrial inputs (mainly river inputs) has remained nearly constant during geological history and is comparable to the mean  $\delta^{98/95}\text{Mo}$  value of continental rocks ( $\sim 0\%$ ) [19,35]. However, the variations in Mo isotopic compositions of rivers, the main contributor to the oceans are poorly constrained, which has important influences on using the Mo isotope to model the redox history. Pearce et al. [16] suggested that both of the dissolved Mo and the released Mo from the suspended load may have a significant consequence on  $\delta^{98/95}\text{Mo}_{\text{seawater}}$ , while the released Mo from colloidal phase is unlikely to significantly affect the Mo isotopic composition of seawater due to the small proportion (<3%) of colloidal Mo in river water. Therefore, the previous assumption is challenged by the higher  $\delta^{98/95}\text{Mo}$  (0.15–2.40‰) observed in several globally significant rivers [15,16,19,21,33,34]. The similar results of higher dissolved  $\delta^{98/95}\text{Mo}$  are also observed in upper XJR (0.51–1.78‰), which could be exported to the lower XJR and then to the South China Sea (SCS).

Moreover, although the proportion of particulate Mo in total Mo in upper XJR (11%) [29] is slightly higher than that in other large rivers (e.g., Yangtze River, 1–7%) [19], the dissolved Mo dominates the river Mo exports and further controls the budget of Mo isotope to the oceans.

By taking the median concentrations of the dissolved Mo (7.3 nmol/L) and the annual average discharge of  $6.47 \times 10^{10}$  m<sup>3</sup>/a for the upper XJR that is obtained from the River and Sediment Bulletin of China (<http://www.mwr.gov.cn/sj/tjgb/zghlnsgb/>), river flux of dissolved Mo to the SCS is calculated as  $\sim 4.72 \times 10^5$  mol/year, which is equivalent to 0.26% of the estimated Mo flux of global river ( $1.8 \times 10^8$  mol/year) [59]. The flux of dissolved Mo with a confirmed isotopically heavy  $\delta^{98/95}\text{Mo}$  value (1.03‰) demonstrates that the isotopic composition of fluvial Mo entering the oceans is likely to be underestimated and the Mo isotope studies of terrestrial river inputs to the ocean should be taken into consideration in future, including karstic rivers.

## 5. Conclusions

In conclusion, this study analyzed the concentrations and isotopic composition of Mo in both the wet and dry season from the upper Xijiang River draining the carbonate terrain, southwest China, to investigate the seasonal variations in the isotopic composition of Mo and the associated mechanisms. Our results show that the dissolved Mo concentrations vary from 5.3–18.9 nmol/L and the  $\delta^{98/95}\text{Mo}$  values vary from 0.51‰ to 1.78‰. The  $\delta^{98/95}\text{Mo}$  values are slightly increased along the main stream and the  $\delta^{98/95}\text{Mo}$  values are higher in the dry season but lower in the wet season in NPR (Nanpanjiang River) reach and BPR (Beipanjiang River) reach. These seasonal and spatial variations can be attributed to both variations in Mo sources and the potential isotope fractionation processes. The seasonal contributions of the weathering of carbonates and sulfide/sulfate minerals are the main sources of the dissolved Mo in the upper XJR. Moreover, we also conclude that there is neither a significant long-term storage of lighter Mo in soils accompanying the weathering processes nor a significant Mo isotopic fractionation during riverine transportation, but the isotopically heavy Mo entering the oceans could significantly impact the reconstruction of redox history of oceans by Mo isotope model.

**Author Contributions:** Conceptualization, G.H.; methodology, G.H. and J.-M.Z.; software, J.Z.; investigation, G.H.; data curation, J.Z., G.H. and J.-M.Z.; writing—original draft, J.Z. and G.H.; writing—review and editing, J.Z. and G.H.

**Funding:** This work was supported by the National Natural Science Foundation of China (Grant No.41325010; 41661144029).

**Acknowledgments:** The authors gratefully acknowledged Fushan Li and Yiliang Hou for field sampling.

**Conflicts of Interest:** The authors declare no conflict of interest.

## References

1. Barbieri, M. Isotopes in Hydrology and Hydrogeology. *Water* **2019**, *11*, 291.
2. Han, G.; Lv, P.; Tang, Y.; Song, Z. Spatial and temporal variation of H and O isotopic compositions of the Xijiang River system, Southwest China. *Isot. Environ. Health Stud.* **2018**, *54*, 137–146. [[CrossRef](#)] [[PubMed](#)]
3. Yang, K.; Han, G.; Liu, M.; Li, X.; Liu, J.; Zhang, Q. Spatial and Seasonal Variation of O and H Isotopes in the Jiulong River, Southeast China. *Water* **2018**, *10*, 1677. [[CrossRef](#)]
4. Wang, W.; Li, S.-L.; Zhong, J.; Li, C.; Yi, Y.; Chen, S.; Ren, Y. Understanding transport and transformation of dissolved inorganic carbon (DIC) in the reservoir system using  $\delta^{13}\text{CDIC}$  and water chemistry. *J. Hydrol.* **2019**, *574*, 193–201. [[CrossRef](#)]
5. Wang, X.; Qiao, W.; Chen, J.; Liu, X.; Yang, F. Understanding the Burial and Migration Characteristics of Deep Geothermal Water Using Hydrogen, Oxygen and Inorganic Carbon Isotopes. *Water* **2018**, *10*, 7. [[CrossRef](#)]
6. Boschetti, T.; Awaleh, M.O.; Barbieri, M. Waters from the Djiboutian Afar: A Review of Strontium Isotopic Composition and a Comparison with Ethiopian Waters and Red Sea Brines. *Water* **2018**, *10*, 1700. [[CrossRef](#)]
7. Han, G.; Tang, Y.; Xu, Z. Fluvial geochemistry of rivers draining karst terrain in Southwest China. *J. Asian Earth Sci.* **2010**, *38*, 65–75. [[CrossRef](#)]

8. Zhang, X.; Xu, Z.; Liu, W.; Moon, S.; Zhao, T.; Zhou, X.; Zhang, J.; Wu, Y.; Jiang, H.; Zhou, L. Hydro-Geochemical and Sr Isotope Characteristics of the Yalong River Basin, Eastern Tibetan Plateau: Implications for Chemical Weathering and Controlling Factors. *Geochem. Geophys. Geosyst.* **2019**, *20*, 1221–1239. [[CrossRef](#)]
9. Wu, W.; Sun, M.; Ji, X.; Qu, S. Sr isotopic characteristics and fractionation during weathering of a small granitic watershed system in the Jiuhua Mountains (eastern China). *J. Hydrol.* **2019**, *568*, 135–146. [[CrossRef](#)]
10. Li, C.; Li, S.-L.; Yue, F.-J.; Liu, J.; Zhong, J.; Yan, Z.-F.; Zhang, R.-C.; Wang, Z.-J.; Xu, S. Identification of sources and transformations of nitrate in the Xijiang River using nitrate isotopes and Bayesian model. *Sci. Total Environ.* **2019**, *646*, 801–810. [[CrossRef](#)]
11. Yue, F.-J.; Liu, C.-Q.; Li, S.-L.; Zhao, Z.-Q.; Liu, X.-L.; Ding, H.; Liu, B.-J.; Zhong, J. Analysis of  $\delta^{15}\text{N}$  and  $\delta^{18}\text{O}$  to identify nitrate sources and transformations in Songhua River, Northeast China. *J. Hydrol.* **2014**, *519*, 329–339. [[CrossRef](#)]
12. Peters, M.; Guo, Q.; Strauss, H.; Wei, R.; Li, S.; Yue, F. Contamination patterns in river water from rural Beijing: A hydrochemical and multiple stable isotope study. *Sci. Total Environ.* **2019**, *654*, 226–236. [[CrossRef](#)]
13. Jiménez-Madrid, A.; Castaño, S.; Vadillo, I.; Martínez, C.; Carrasco, F.; Soler, A. Applications of Hydro-Chemical and Isotopic Tools to Improve Definitions of Groundwater Catchment Zones in a Karstic Aquifer: A Case Study. *Water* **2017**, *9*, 595. [[CrossRef](#)]
14. Moore, L.J.; Machlan, L.A.; Shields, W.R.; Garner, E.L. Internal normalization techniques for high accuracy isotope dilution analyses. Application to molybdenum and nickel in standard reference materials. *Anal. Chem.* **1974**, *46*, 1082–1089. [[CrossRef](#)]
15. Wang, Z.; Ma, J.; Li, J.; Wei, G.; Chen, X.; Deng, W.; Xie, L.; Lu, W.; Zou, L. Chemical weathering controls on variations in the molybdenum isotopic composition of river water: Evidence from large rivers in China. *Chem. Geol.* **2015**, *410*, 201–212. [[CrossRef](#)]
16. Pearce, C.R.; Burton, K.W.; von Strandmann, P.A.E.P.; James, R.H.; Gíslason, S.R. Molybdenum isotope behaviour accompanying weathering and riverine transport in a basaltic terrain. *Earth Planet. Sci. Lett.* **2010**, *295*, 104–114. [[CrossRef](#)]
17. Wille, M.; Kramers, J.D.; Nägler, T.F.; Beukes, N.J.; Schröder, S.; Meisel, T.; Lacassie, J.P.; Voegelin, A.R. Evidence for a gradual rise of oxygen between 2.6 and 2.5Ga from Mo isotopes and Re-PGE signatures in shales. *Geochim. Cosmochim. Acta* **2007**, *71*, 2417–2435. [[CrossRef](#)]
18. Wille, M.; Naegler, T.F.; Lehmann, B.; Schroeder, S.; Kramers, J.D. Hydrogen sulphide release to surface waters at the Precambrian/Cambrian boundary. *Nature* **2008**, *453*, 767–769. [[CrossRef](#)] [[PubMed](#)]
19. Archer, C.; Vance, D. The isotopic signature of the global riverine molybdenum flux and anoxia in the ancient oceans. *Nat. Geosci.* **2008**, *1*, 597–600. [[CrossRef](#)]
20. Wang, Z.; Ma, J.; Li, J.; Wei, G.; Zeng, T.; Li, L.; Zhang, L.; Deng, W.; Xie, L.; Liu, Z. Fe (hydro) oxide controls Mo isotope fractionation during the weathering of granite. *Geochim. Cosmochim. Acta* **2018**, *226*, 1–17. [[CrossRef](#)]
21. Neubert, N.; Heri, A.R.; Voegelin, A.R.; Nägler, T.F.; Schlunegger, F.; Villa, I.M. The molybdenum isotopic composition in river water: Constraints from small catchments. *Earth Planet. Sci. Lett.* **2011**, *304*, 180–190. [[CrossRef](#)]
22. Hammond, C.R. The Elements. In *CRC Handbook of Chemistry and Physics*; Lide, D.R., Ed.; CRC Press: Boca Raton, FL, USA, 2005.
23. Xu, Z.; Liu, C.Q. Chemical weathering in the upper reaches of Xijiang River draining the Yunnan–Guizhou Plateau, Southwest China. *Chem. Geol.* **2007**, *239*, 83–95. [[CrossRef](#)]
24. Li, S.-L.; Calmels, D.; Han, G.; Gaillardet, J.; Liu, C.-Q. Sulfuric acid as an agent of carbonate weathering constrained by  $\delta^{13}\text{CDIC}$ : Examples from Southwest China. *Earth Planet. Sci. Lett.* **2008**, *270*, 189–199. [[CrossRef](#)]
25. Han, G.; Liu, C.-Q. Water geochemistry controlled by carbonate dissolution: A study of the river waters draining karst-dominated terrain, Guizhou Province, China. *Chem. Geol.* **2004**, *204*, 1–21. [[CrossRef](#)]
26. Wu, Q.; Han, G.; Li, F.; Tang, Y. Characteristic and source analysis of major ions in Nanpanjiang and Beipanjiang at the upper Pearl River during the wet season. *Environ. Chem.* **2015**, *34*, 1289–1296. (In Chinese)
27. Ma, K.; Wu, Q.; Han, G.; Dong, A. Hydrochemical characteristics and sources of Nanpanjiang and Beipanjiang river basins during dry seasons. *Carsol. Sin.* **2018**, *37*, 192–202. (In Chinese)
28. Liu, J.; Li, S.-L.; Chen, J.-B.; Zhong, J.; Yue, F.-J.; Lang, Y.; Ding, H. Temporal transport of major and trace elements in the upper reaches of the Xijiang River, SW China. *Environ. Earth Sci.* **2017**, *76*, 299. [[CrossRef](#)]

29. Zeng, J.; Han, G.; Wu, Q.; Tang, Y. Geochemical characteristics of dissolved heavy metals in Zhujiang River, Southwest China: Spatial-temporal distribution, source, export flux estimation and a water quality assessment. *PeerJ* **2019**, *7*, e6578. [[CrossRef](#)]
30. Li, J.; Liang, X.-R.; Zhong, L.-F.; Wang, X.-C.; Ren, Z.-Y.; Sun, S.-L.; Zhang, Z.-F.; Xu, J.-F. Measurement of the Isotopic Composition of Molybdenum in Geological Samples by MC-ICP-MS using a Novel Chromatographic Extraction Technique. *Geostand. Geoanal. Res.* **2014**, *38*, 345–354. [[CrossRef](#)]
31. Gaillardet, J.; Viers, J.; Dupré, B. Trace Elements in River Waters. In *Treatise on Geochemistry*, 2nd ed.; Holland, H.D., Turekian, K.K., Eds.; Elsevier: Oxford, UK, 2014; pp. 195–235.
32. Li, S.; Zhang, Q. Spatial characterization of dissolved trace elements and heavy metals in the upper Han River (China) using multivariate statistical techniques. *J. Hazard. Mater.* **2010**, *176*, 579–588. [[CrossRef](#)]
33. Rahaman, W.; Goswami, V.; Singh, S.K.; Rai, V.K. Molybdenum isotopes in two Indian estuaries: Mixing characteristics and input to oceans. *Geochim. Cosmochim. Acta* **2014**, *141*, 407–422. [[CrossRef](#)]
34. Voegelin, A.R.; Nägler, T.F.; Pettke, T.; Neubert, N.; Steinmann, M.; Pourret, O.; Villa, I.M. The impact of igneous bedrock weathering on the Mo isotopic composition of stream waters: Natural samples and laboratory experiments. *Geochim. Cosmochim. Acta* **2012**, *86*, 150–165. [[CrossRef](#)]
35. Siebert, C.; Nägler, T.F.; von Blanckenburg, F.; Kramers, J.D. Molybdenum isotope records as a potential new proxy for paleoceanography. *Earth Planet. Sci. Lett.* **2003**, *211*, 159–171. [[CrossRef](#)]
36. An, H. Remote sensing survey and analysis of current land utilization in the drainage area of Nanpanjiang and Beipanjiang rivers in Guizhou province. *Guizhou Geol.* **1996**, *13*, 344–349. (In Chinese)
37. Tang, Y.; Han, G.L.; Li, F.S.; Wu, Q.X. Natural and anthropogenic sources of atmospheric dust at a remote forest area in Guizhou karst region, southwest China. *Geochem.-Explor. Environ. Anal.* **2016**, *16*, 159–163. [[CrossRef](#)]
38. Tang, Y.; Han, G. Seasonal Variation and Quality Assessment of the Major and Trace Elements of Atmospheric Dust in a Typical Karst City, Southwest China. *Int. J. Environ. Res. Public Health* **2019**, *16*, 325. [[CrossRef](#)] [[PubMed](#)]
39. Han, G.; Wu, Q.; Tang, Y. Acid rain and alkalization in southwestern China: Chemical and strontium isotope evidence in rainwater from Guiyang. *J. Atmos. Chem.* **2011**, *68*, 139–155. [[CrossRef](#)]
40. Han, G.; Tang, Y.; Wu, Q.; Tan, Q. Chemical and strontium isotope characterization of rainwater in karst virgin forest, Southwest China. *Atmos. Environ.* **2010**, *44*, 174–181. [[CrossRef](#)]
41. Nie, X.; Wang, Y.; Li, Y.; Sun, L.; Li, T.; Yang, M.; Yang, X.; Wang, W. Characteristics and impacts of trace elements in atmospheric deposition at a high-elevation site, southern China. *Environ. Sci. Pollut. Res.* **2017**, *24*, 22839–22851. [[CrossRef](#)]
42. Huang, S.; Tu, J.; Liu, H.; Hua, M.; Liao, Q.; Feng, J.; Weng, Z.; Huang, G. Multivariate analysis of trace element concentrations in atmospheric deposition in the Yangtze River Delta, East China. *Atmos. Environ.* **2009**, *43*, 5781–5790. [[CrossRef](#)]
43. Zheng, X.; Guo, X.; Zhao, W.; Shu, T.; Xin, Y.; Yan, X.; Xiong, Q.; Chen, F.; Lv, M. Spatial variation and provenance of atmospheric trace elemental deposition in Beijing. *Atmos. Pollut. Res.* **2016**, *7*, 260–267. [[CrossRef](#)]
44. Lyu, Y.; Zhang, K.; Chai, F.; Cheng, T.; Yang, Q.; Zheng, Z.; Li, X. Atmospheric size-resolved trace elements in a city affected by non-ferrous metal smelting: Indications of respiratory deposition and health risk. *Environ. Pollut.* **2017**, *224*, 559–571. [[CrossRef](#)]
45. Lee, P.-K.; Choi, B.-Y.; Kang, M.-J. Assessment of mobility and bio-availability of heavy metals in dry depositions of Asian dust and implications for environmental risk. *Chemosphere* **2015**, *119*, 1411–1421. [[CrossRef](#)]
46. Liu, J.; Li, S.; Zhong, J.; Zhu, X.; Guo, Q.; Lang, Y.; Han, X. Sulfate sources constrained by sulfur and oxygen isotopic compositions in the upper reaches of the Xijiang River, China. *Acta Geochim.* **2017**, *36*, 611–618. [[CrossRef](#)]
47. Gaillardet, J.; Dupré, B.; Louvat, P.; Allègre, C.J. Global silicate weathering and CO<sub>2</sub> consumption rates deduced from the chemistry of large rivers. *Chem. Geol.* **1999**, *159*, 3–30. [[CrossRef](#)]
48. Lü, P.; Han, G.; Wu, Q. Chemical characteristics of rainwater in karst rural areas, Guizhou Province, Southwest China. *Acta Geochim.* **2017**, *36*, 572–576. [[CrossRef](#)]
49. Wu, Q.; Han, G.; Tao, F.; Tang, Y. Chemical composition of rainwater in a karstic agricultural area, Southwest China: The impact of urbanization. *Atmos. Res.* **2012**, *111*, 71–78. [[CrossRef](#)]

50. Xu, L.; Lehmann, B.; Mao, J. Seawater contribution to polymetallic Ni–Mo–PGE–Au mineralization in Early Cambrian black shales of South China: Evidence from Mo isotope, PGE, trace element and REE geochemistry. *Ore Geol. Rev.* **2013**, *52*, 66–84. [[CrossRef](#)]
51. Voegelin, A.R.; Nägler, T.F.; Samankassou, E.; Villa, I.M. Molybdenum isotopic composition of modern and Carboniferous carbonates. *Chem. Geol.* **2009**, *265*, 488–498. [[CrossRef](#)]
52. Goldberg, T.; Archer, C.; Vance, D.; Poulton, S.W. Mo isotope fractionation during adsorption to Fe (oxyhydr)oxides. *Geochim. Cosmochim. Acta* **2009**, *73*, 6502–6516. [[CrossRef](#)]
53. Siebert, C.; Pett-Ridge, J.C.; Opfergelt, S.; Guicharnaud, R.A.; Halliday, A.N.; Burton, K.W. Molybdenum isotope fractionation in soils: Influence of redox conditions, organic matter and atmospheric inputs. *Geochim. Cosmochim. Acta* **2015**, *162*, 1–24. [[CrossRef](#)]
54. Dai, Q.; Liu, Z.; Shao, H.; Yang, Z. Karst bare slope soil erosion and soil quality: A simulation case study. *Solid Earth* **2015**, *6*, 985–995. [[CrossRef](#)]
55. Dai, Q.H.; Peng, X.D.; Wang, P.J.; Li, C.L.; Shao, H.B. Surface erosion and underground leakage of yellow soil on slopes in karst regions of southwest China. *Land Degrad. Dev.* **2018**, *29*, 2438–2448. [[CrossRef](#)]
56. An, Y.; Hou, Y.; Wu, Q.; Qing, L.; Li, L. Chemical weathering and CO<sub>2</sub> consumption of a high-erosion-rate karstic river: A case study of the Sanchahe River, southwest China. *Chin. J. Geochem.* **2015**, *34*, 601–609. [[CrossRef](#)]
57. Zeng, J.; Han, G.; Wu, Q.; Tang, Y. Heavy Metals in Suspended Particulate Matter of Zhujiang River, Southwest China: Contents, Sources and Health Risks. *Int. J. Environ. Res. Public Health* **2019**, *94*, e94145.
58. Zou, J. Geochemical characteristics and organic carbon sources within the upper reaches of the Xi River, southwest China during high flow. *J. Earth Syst. Sci.* **2017**, *126*, 6. [[CrossRef](#)]
59. McManus, J.; Berelson, W.M.; Severmann, S.; Poulson, R.L.; Hammond, D.E.; Klinkhammer, G.P.; Holm, C. Molybdenum and uranium geochemistry in continental margin sediments: Paleoproxy potential. *Geochim. Cosmochim. Acta* **2006**, *70*, 4643–4662. [[CrossRef](#)]



© 2019 by the authors. Licensee MDPI, Basel, Switzerland. This article is an open access article distributed under the terms and conditions of the Creative Commons Attribution (CC BY) license (<http://creativecommons.org/licenses/by/4.0/>).